Hybrid dielectric and iris-loaded periodic accelerating structure

Peng Zou, Liling Xiao, Xiang Sun, and Wei Gai[a)]
Argonne National Laboratory, Argonne, Illinois 60439

Thomas Wong
Illinois Institute of Technology, Chicago, Illinois 60616

(Received 1 February 2001; accepted for publication 10 May 2001)

One disadvantage of conventional iris-loaded accelerating structures is the high ratio of the peak surface electric field to the peak axial electric field useful for accelerating a beam. Typically this ratio $E_s/E_a \geqslant 2$. The high surface electric field relative to the accelerating gradient may prove to be a limitation for realizing technologies for very high gradient accelerators. In this article, we present a scheme that uses a hybrid dielectric and iris-loaded periodic structure to reduce E_s/E_a to near unity, while the shunt impedance per unit length r and the quality factor Q compare favorably with conventional metallic structures. The analysis based on MAFIA simulations of such structures shows that we can lower the peak surface electric field close to the accelerating gradient while maintaining high acceleration efficiency as measured by r/Q. Numerical examples of X-band hybrid accelerating structures are given.
[DOI: 10.1063/1.1383578]

I. INTRODUCTION

One of the major challenges confronting future high energy linear accelerators is the development of high gradient accelerating structures. The most commonly studied structure is a conventional iris-loaded copper structure representing an evolution from those used at SLAC/SLC to the proposed NLC and possibly CLIC.[1–3] However, in all the iris-loaded structures, the peak surface electric field E_s can be an important constraint in such high energy accelerating structure design because it is, in general, found to be a factor of 2 larger than the axial acceleration field E_a.[1–4] Because the peak surface electric field causes breakdown of the structure, it represents a direct limitation on the maximum acceleration gradient that can be obtained. If the peak surface electric field exceeds the breakdown limit at the operating frequency, it can cause damage to the irises through arcing and detune the structure. Thus, the high ratio of E_s to E_a limits the achievable accelerating gradient, assuming the availability of high power rf sources is not a constraint here. In this article, we propose a hybrid dielectric and iris-loaded acceleration structure that has a lower ratio of E_s to E_a, and comparable shunt impedance per unit length r and r/Q with a conventional iris-loaded accelerating structure. Using this device E_s/E_a can be reduced to about 1, while maintaining reasonably good acceleration efficiency as measured by r and r/Q. The upper limit of the accelerating gradient can be increased depending on the dielectric breakdown properties at high fields.

The use of uniform dielectric-lined circular waveguides as accelerating structures has been discussed in many previous studies.[5–8] One distinct advantage is that the axial accelerating electric field is the maximum field in this class of structure. The acceleration mode used here is the TM_{01}. The group velocity is typically less than 10% of the speed of light. Such small group velocities can be obtained by the use of high dielectric constant ceramics which, however, have the drawback of an enhanced peak surface magnetic field which results in more power dissipation on the wall. The result is that the quality factor Q of a dielectric-lined waveguide is degraded compared to an iris-loaded structure with the same group velocity.

Based on these observations we might consider a hybrid dielectric and iris-loaded structure in order to produce a device which balances high Q and reduced surface fields. This device is shown in Fig. 1. Calculations of the properties of a hybrid traveling-wave acceleration structure at 11.4 GHz as a function of iris size and permittivity of the loading dielectric are performed. We show that it is indeed possible to significantly reduce the ratio of the peak surface electric field to the accelerating field gradient without diminishing to any great extent the shunt impedance per unit length r and r/Q.

II. NUMERICAL METHOD

One way to study traveling-wave structures is to use a numerical code such as SUPERFISH[9] or MAFIA.[10] These codes provide accurate fields and other electromagnetic properties of a standing wave structure. Loew *et al.*[11] showed that by using rf properties of standing-wave structures, one could obtain rf properties of the corresponding traveling-wave structures. This conversion will be briefly outlined in the following.

Consider a periodic structure as shown in Fig. 1. It is well known that the axial electric field E_z of the TM_{01} mode in the traveling-wave periodic structures can be expressed as

[a)]Electronic mail: wg@hep.anl.gov

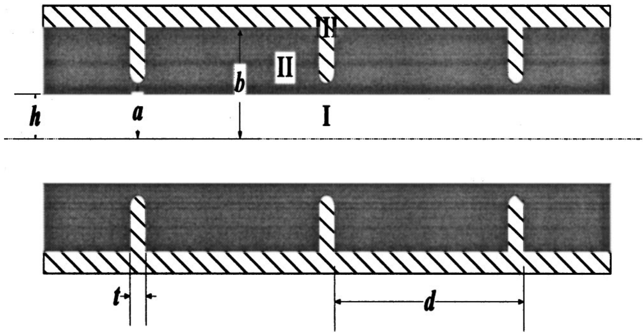

FIG. 1. Schematic drawing of a hybrid dielectric iris-loaded accelerating structure. The function of the dielectric is to reduce the surface electric field on the iris relative to the axial accelerating field. In the figure, region I is vacuum; region II is ceramic with dielectric constant ε; region III is copper. a is the iris radius, b is the outer radius, and h is the beam hole radius. t is the thickness of the iris and d is the length of one cell. In this article, we use a to denote the iris radius for both hybrid dielectric iris-loaded structures and pure iris-loaded structures.

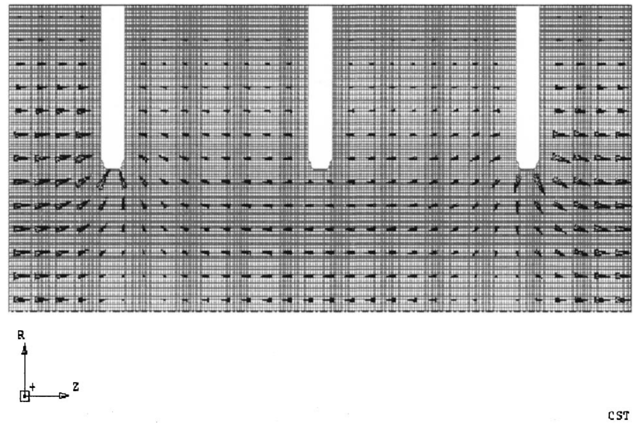

FIG. 2. Electric field pattern of the $2\pi/3$ mode in an iris-loaded accelerating structure. The iris radius $a = 5.6$ mm, the iris thickness $t = 1.0$ mm, and outer radius $b = 11.1254$ mm. Here $E_s/E_a = 2.4$.

$$E_{z,TW} = \sum_{n=-\infty}^{n=+\infty} a_n(r) e^{j(\omega t - \beta_n z)}, \tag{1}$$

where a_n is the amplitude of the space harmonic of index n

$$\beta_n z = \beta_0 z + \frac{2\pi n z}{d}, \tag{2}$$

where β_n is the propagation constant of the space harmonic of index n, and d is the spatial period (the length of one cell). The propagation constant of such a TM_{01} wave is the same as β_0.

With Neumann boundary conditions ($E_t = 0$) applied at $z = 0$ and $z = \lambda$ (where $\lambda = 2\pi/\beta_0$), the axial electric fields of the standing waves can be expressed as

$$E_{z,SW} = e^{j\omega t} \sum_{n=-\infty}^{n=+\infty} 2a_n \cos \beta_n z. \tag{3}$$

The factor of 2 comes from the summation of two traveling waves of amplitude a_n. This equation takes the same form for the other field components.

Using MAFIA, one can calculate resonant frequencies, stored energies, and power dissipation of resonant modes in an array of cavities. The standing-wave field components output by the code can be analyzed as follows to obtain the traveling-wave components.

If two traveling waves of the proper phase can add up to a standing wave [Eq. (3)], there must conversely be two appropriately phased standing waves that add up to a traveling wave. Assuming the first standing wave is $\vec{A}$, and the second standing wave $\vec{B}$ is obtained by shifting $\vec{A}$ to the left by d, then

$$\vec{B} = e^{j\omega t} \sum_{-\infty}^{+\infty} 2a_n \cos \beta_n (z+d), \quad \vec{A} = e^{j\omega t} \sum_{-\infty}^{+\infty} 2a_n \cos \beta_n z. \tag{4}$$

Both of these standing waves are made up of one traveling wave going left and one going right. It is possible to add them with the proper phases to have the traveling waves going left canceled and those going right reinforced and thus obtain the traveling-wave field component in the structure. This can be achieved by multiplying $\vec{A}$ by $e^{j(\beta_0 d - \pi/2)}$ and $\vec{B}$ by $e^{j\pi/2}$, and adding them up. Then we have

$$\vec{B} e^{j\pi/2} + \vec{A} e^{j(\beta_0 d - \pi/2)} = 2 \sin \beta_0 d \sum_{-\infty}^{+\infty} a_n e^{j(\omega t - \beta_n z)}. \tag{5}$$

The amplitude and phase of the field components of traveling waves can be obtained by the following equations:

$$|TW|^2 = \frac{A^2 + B^2 - 2AB \cos \beta_0 d}{4 \sin^2 \beta_0 d}, \qquad \tan \theta(z) = \frac{B - A \cos \beta_0 d}{A \sin \beta_0 d}, \tag{6}$$

where A and B are amplitudes of the standing waves that are functions of z.

The group velocity of a traveling wave can be calculated from the energy velocity $v_g = P/U$,[12] where P is the time average power flow in such structure, and U is the time average of the stored energy per unit length. The shunt impedance per unit length r of a traveling-wave accelerating

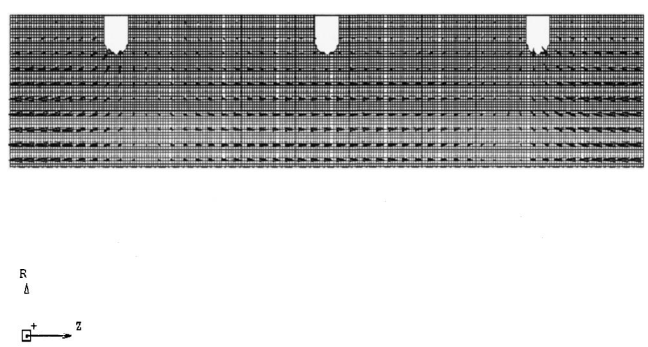

FIG. 3. Electric field pattern of $2\pi/3$ mode in a hybrid dielectric iris-loaded accelerating structure. The $\varepsilon = 6$, $a = 4.0$ mm, $b = 5.361$ mm, and the beam hole radius $h = 2.0$ mm. $E_s/E_a = 1.01$.

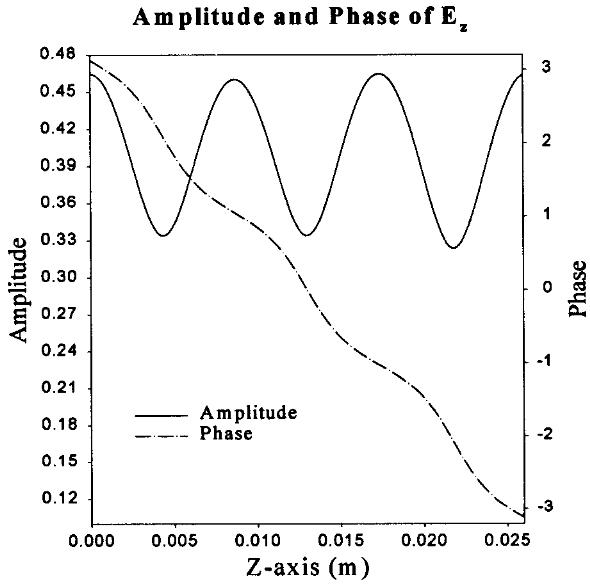

FIG. 4. Amplitude and phase plot of E_z at $r=0$ in a hybrid dielectric iris-loaded traveling-wave structure. The geometric parameters of this structure are given in Fig. 3.

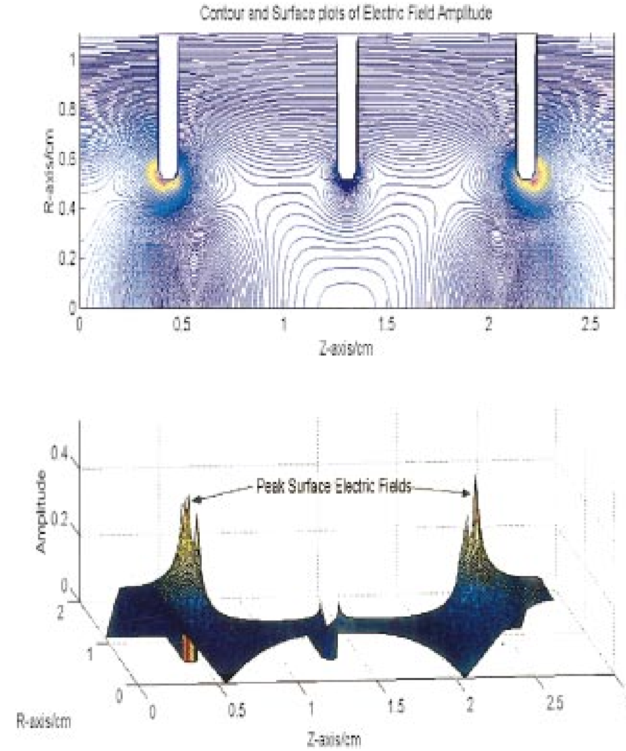

FIG. 5. (Color) The contour plot and corresponding surface plot show the distribution of electric field amplitudes in a pure iris-loaded traveling-wave structure. The geometric parameters of this structure are given in Fig. 2. In both contour plot and surface plot, the dark red indicates the strongest field amplitude. We observe that the strongest electric field occurs at the edge of the iris. In this case, E_s/E_a is about 2.4.

structure, which measures the effectiveness of producing an accelerating gradient for a given power dissipated, is defined by[13]

$$r=\frac{E_a^2}{-dP/dz}=\frac{E_a^2 Q v_g}{\omega P}=\frac{E_a^2 Q}{\omega U}, \tag{7}$$

where E_a is the accelerating field gradient, and $-dP/dz$ is the resistive power dissipation per unit length in the walls of the structure. For traveling-wave structures, E_a is the peak axial electric field. Since we already have the field solutions of the resonator it is easier to obtain r from the effective shunt impedance per unit length of such standing-wave structure r_{SW}. The relation between r and r_{SW} is expressed as simply as $r=2r_{\mathrm{SW}}$.

One can also use $r/Q=E_a^2/\omega U$ to measure the efficiency of acceleration per unit stored energy at a given frequency. It is useful because it is a function only of the cavity geometry and is independent of the surface properties that determine the power losses.

III. NUMERICAL RESULTS

In this article, we specialize our investigation to consider only the $2\pi/3$ mode of the propagated wave, whose wavelength λ is equal to the total length of three cells when the phase velocity is the speed of light as required for the acceleration of ultrarelativistic particles. First, we calculated a resonator with three cells (with Neumann boundaries $E_t=0$ at $z=0$ and $z=\lambda$) using MAFIA. The field solutions and mesh coordinates were output to ASCII data files. A postprocessing program was written to extract the field solutions and mesh information of the standing-wave solution, and then carry out the conversion from standing-wave solutions to traveling-wave solutions using the method outlined in Sec. II.

Figures 2 and 3 show the MAFIA simulation results for the electric field pattern of the $2\pi/3$ mode in a pure iris-loaded structure and a hybrid dielectric iris-loaded structure, respectively. Because of the axial symmetry, only the upper half part of the longitudinal cross section is plotted.

The conversion of standing waves to traveling waves according to Eq. (6) was carried out. Figure 4 shows the amplitude and phase of the axial electric field of the resulting traveling wave in a hybrid dielectric iris-loaded structure (with $a=5.5$ mm, $b=6.923$ mm, and $h=4$ mm). Other field components can be obtained through a similar procedure.

A. Calculation of pure iris-loaded traveling-wave structures

The corresponding traveling-wave parameters of Fig. 2 structure were calculated and given below in Table I. In a pure iris-loaded structure, the group velocity of the TM_{01} wave and shunt impedance per unit length are determined by

TABLE I. 11.424 GHz pure iris-loaded traveling-wave structure.

a (mm)	b (mm)	t (mm)	d (mm)	E_s/E_a	r (MΩ/m)	Q	r/Q (Ω/m)	v_g (c)
5.6021	11.1254	1.0	8.7535	2.4	75.6	7251	10 343	0.088

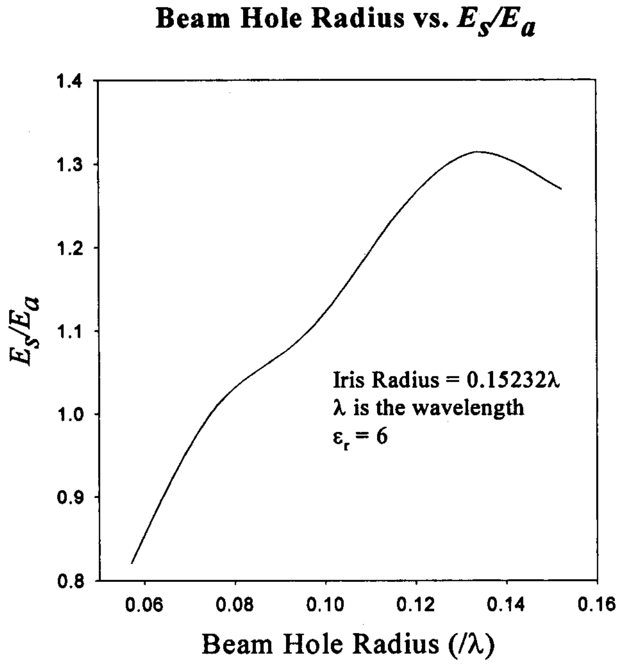

FIG. 6. Beam hole radius h vs E_s/E_a in a hybrid dielectric iris-loaded structure. Here $\varepsilon=6$, and the iris radius a is fixed as 4.0 mm. The wavelength λ is equal to the total length of three cells, and is 26.2605 mm. In all calculations, the iris thickness t is fixed as 1.0 mm. The outer radius b is adjusted accordingly to have the phase velocity of the TM_{01} mode equal to c.

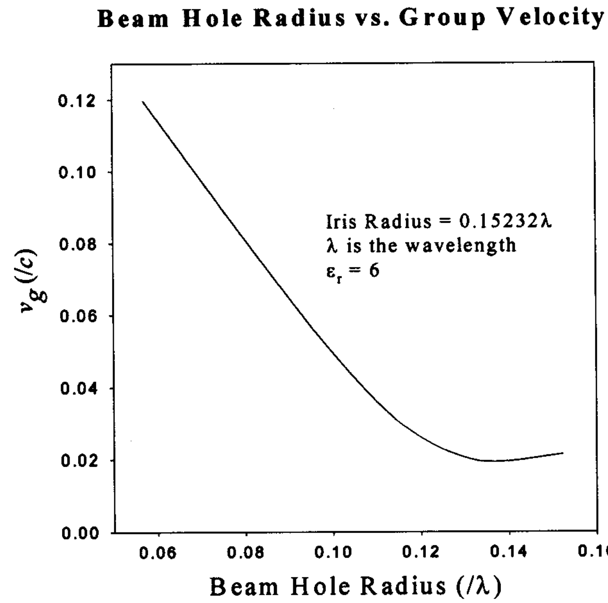

FIG. 7. Beam hole radius vs group velocity in a hybrid dielectric iris-loaded structure with geometry as in Fig. 6.

the radius of the irises. Meanwhile, the outer radius of the cylinder has to be adjusted to maintain the phase velocity of the TM_{01} wave synchronized with the beam velocity c. Thus, the iris radius is the governing geometric parameter for the rf properties of a pure iris-loaded accelerating structure. For the structure with iris radius $a=5.6$ mm, resulting in a group velocity of $0.088c$. The shunt impedance per unit length r is 75 MΩ/m, and the quality factor Q is 7251.

The contour plot and surface plot of the distribution of electric field amplitude are shown in Fig. 5. We can easily identify that the peak surface electric field occurs at the edge of the iris, and E_s/E_a is about 2.4.

B. Calculation of hybrid dielectric iris-loaded traveling-wave structures

Unlike pure iris-loaded structure, the group velocity and shunt impedance per unit length r of acceleration TM_{01} mode in a hybrid dielectric iris-loaded structure is not only the function of beam hole radius, but also iris radius and dielectric constant. For a given group velocity, the outer radius of the cylinder b is determined to synchronize the phase velocity with the beam velocity. In this section, we give a self-consistent calculation of hybrid structures with a fixed iris radius and a range of dielectric constant ε, and also varying the beam hole radius.

To illustrate our point, we have chosen $\varepsilon=6$ as our first example. Figure 6 shows E_s/E_a as the function of beam hole radius. Its value ranges from 0.8 to 1.5, significantly lower than the pure iris-loaded structure case described in Fig. 2. Figure 7 shows the effect of the beam hole radius on the group velocity of the TM_{01} mode for the same structure parameters. In order to have a fair comparison for all the parameters studied here, we have chosen the group velocity to be nearly the same as in the pure iris loaded case. Table II gives the geometric parameters and rf properties of a hybrid structures for two different beam hole sizes. The first case, with beam hole radius of 4 mm and iris radius of 5.5 mm, gives a shunt impedance of 38 MΩ/m with $Q=4506$. One could decrease the beam hole to increase the shunt impedance and Q as shown in the second case of Table II. The ratio $E_s/E_a=1.01$ is obtained. For a beam hole radius = 2 mm and adjusting the other parameters accordingly, we obtain $r=66\,\mathrm{M}\,\Omega/\mathrm{m}$, slightly lower than that of the pure iris-loaded structure listed in Table I. Meanwhile, the quality factor $Q=4899$ is about 30% lower than the pure iris-loaded case due to the increased surface magnetic fields. However, the acceleration efficiency measured by r/Q is also improved by 30% and $E_s/E_a\approx1$. Figure 8 shows the contour plot and surface plot of electric field distribution in the hybrid structure given in Table II. It shows that the peak surface electric field is

TABLE II. 11.424 GHz hybrid dielectric iris-loaded traveling-wave structure ($\varepsilon=6, t=1.0$ mm).

a (mm)	b (mm)	k (mm)	d (mm)	E_s/E_a	r (MΩ/m)	Q	r/Q (Ω/m)	v_g (c)
5.5	6.923	4.0	8.7535	1.1	38.0	4506.0	8433.2	0.089
4.0	5.361	2.0	8.7535	1.01	66.8	4899.0	13635.4	0.087

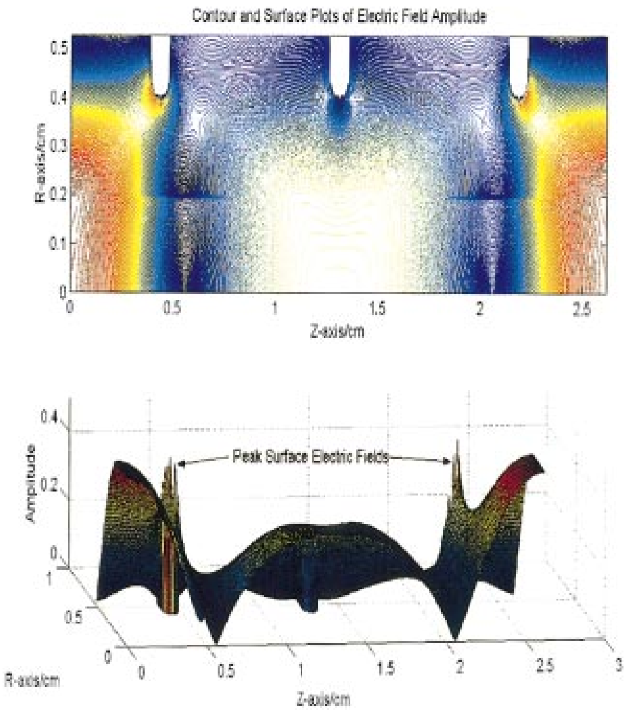

FIG. 8. (Color) Contour and surface plots showing the distribution of electric field amplitude in a hybrid dielectric iris-loaded traveling-wave structure. The parameters of this structure are given in Fig. 3. In both plots, the dark red indicates the strongest field amplitude. We can see the strongest electric field on the iris surface is about the same as the axial electric field in this case: E_s/E_a is about 1.01.

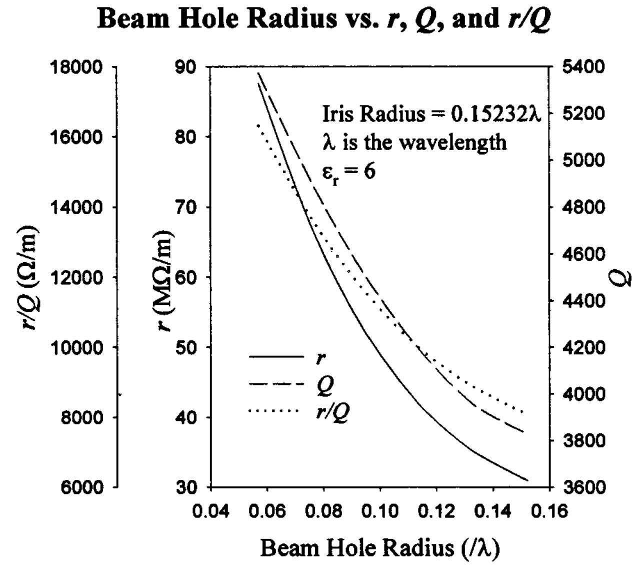

FIG. 9. Shunt impedance, normalized shunt impedance, and quality factor of the hybrid dielectric iris-loaded structure as functions of the beam hole radius h. Device geometry as in Fig. 6.

reduced to the same magnitude as the peak axial electric field. Therefore, hybrid dielectric iris-loaded structures reduce the peak surface electric field with comparable r/Q to iris-loaded structures. However, one should notice that the contact between the irises and the dielectric must be as close as possible. One might expect that if there is a large gap existing between a metallic iris and dielectric resulting from fabrication, and then the electric fields on the irises could be enhanced. From qualitative analysis, the surface electric field on the iris will go up as the gap increases. Detail study of this effect should be investigated in the future, and other engineering issues should also be addressed.

Although we could lower the E_s/E_a by introducing dielectric loading into the structure we have to encounter another unknown problem: dielectric breakdown under high frequency rf fields. The dielectric breakdown limit becomes the constraint of the maximum achievable accelerating gradient instead of the surface breakdown limit of copper in pure iris-loaded structures. Dielectric breakdown at various frequencies has been studied in wakefield acceleration experiments,[14] and showed no sign of breakdown up to 20 MV/m at 15 GHz. Besides dielectric breakdown limit, other mostly unknown factors, such as Joule heating and vacuum properties of dielectric loaded structures under high rf power, should also be weighed in to evaluate this type of hybrid dielectric iris-loaded structure. With a recently proposed experiment,[15] breakdown phenomena can be explored at 50–70 MV/m field strengths, approaching the NLC desired gradient. Moreover, Joule heating and vacuum properties will also be investigated. If dielectrics can maintain these field magnitudes, then the scheme we analyzed in the article would provide an alternate approach that lowers the peak field on the iris by more than a factor of two. This may be an important factor for realizing accelerating structures for very high gradient accelerators.

The variation of shunt impedance per unit length r, r/Q, and quality factor Q as the functions of the beam hole radius are shown in Fig. 9. For a fixed iris radius and dielectric

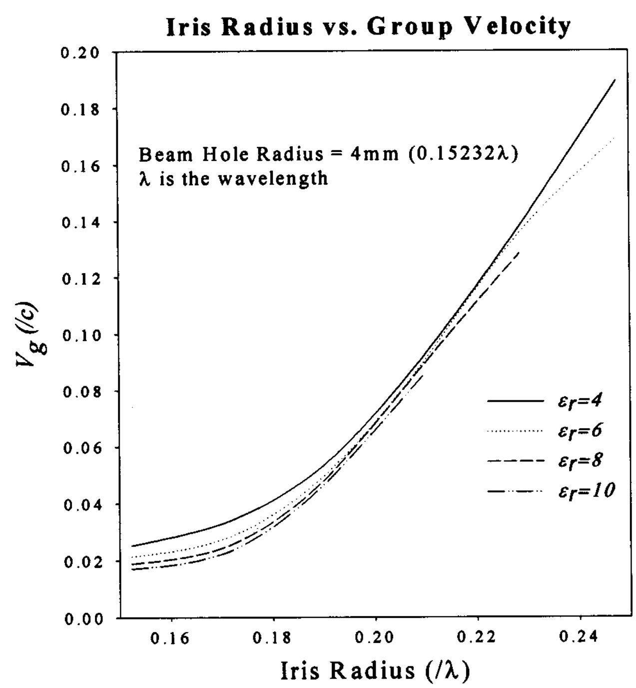

FIG. 10. Iris radius a vs v_g for $2\pi/3$ mode in a hybrid dielectric iris-loaded structure, when the beam hole radius h is fixed as 4.0 mm, and the wavelength λ is 26.2605 mm. Varying the dielectric constant of the loading ceramics ε and iris radius a, the outer radius b is adjusted accordingly to have the phase velocity of TM_{01} mode synchronized with the speed of light c.

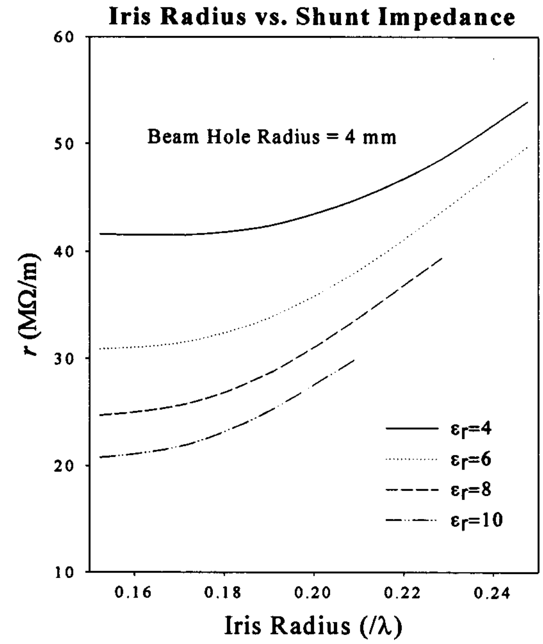

FIG. 11. The shunt impedance per unit length r of $2\pi/3$ luminal mode in a hybrid dielectric iris-loaded structure, when the beam hole radius h is fixed as 4.0 mm, and the wavelength λ is 26.2605 mm.

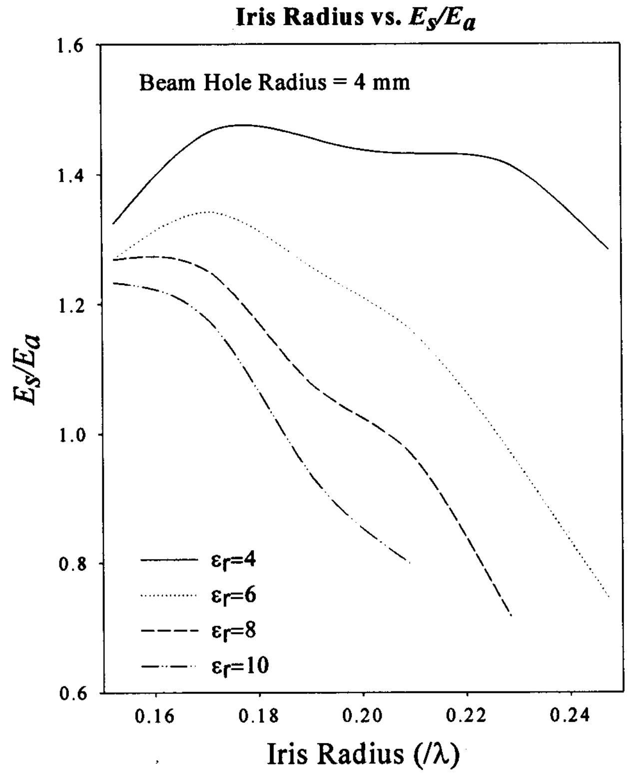

FIG. 13. The ratio E_s/E_a of the luminal $2\pi/3$ mode as a function of iris radius a and dielectric constant ε in the hybrid dielectric iris-loaded structure. All other structure parameters as in previous figures.

constant, a smaller beam hole radius is preferred for achieving higher acceleration efficiency and less power dissipation on the wall.

The overall optimization of the parameters is complicated because we have to consider three variables: ε, a, and b. Iris thickness t and the beam hole radius are assumed fixed for the following calculation. The beam hole radius was chosen as 0.15λ or 4 mm. Figure 10 shows iris radius versus group velocity for several dielectric constants. The results indicate the group velocity is mostly determined by the size of iris, not ε. Figures 11 and 12 show r and Q as a function of a and ε. The high ε gives lower Q. Therefore, the optimal ε for this structure is between 4 and 6.

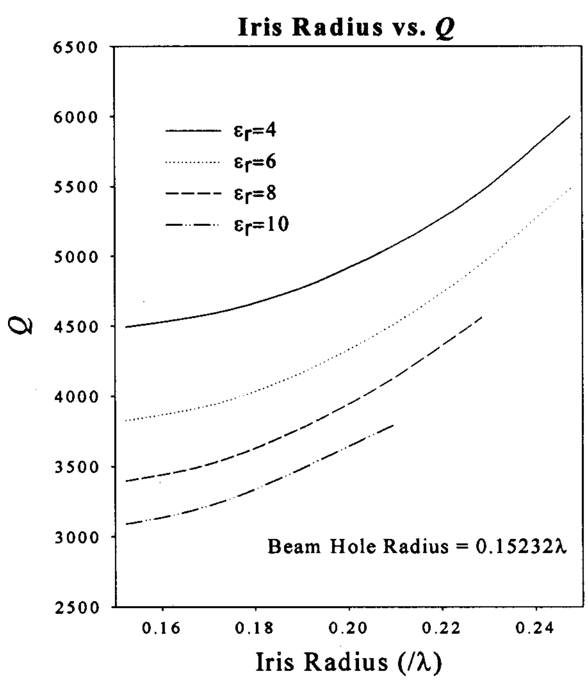

FIG. 12. The quality factor Q of $2\pi/3$ luminal mode as a function of iris radius a and dielectric constant ε in the hybrid dielectric iris-loaded structure, when the beam hole radius h is fixed as 4.0 mm, and the wavelength λ is 26.2605 mm.

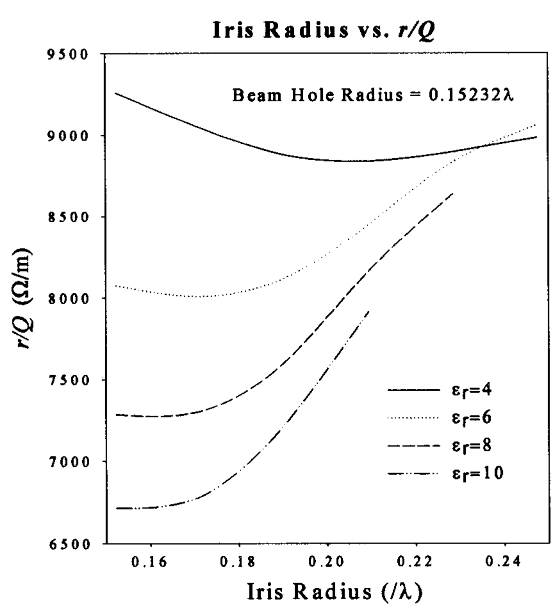

FIG. 14. r/Q of the $2\pi/3$ mode as a function of iris radius a and dielectric constant ε in the hybrid dielectric iris-loaded structures.

The variation of the ratio of the peak surface electric field to the peak accelerating gradient in these given examples is shown in Fig. 13. As shown, high ε can reduce the ratio E_s/E_a significantly as expected. The r/Q plots are given in Fig. 14. If the dielectric constant is chosen between 4 and 6 for the given geometric parameters, r/Q can be maintained at relatively high constant value.

IV. CONCLUSION

The analysis of hybrid dielectric loaded periodic accelerating structures shows that the peak surface electric field can be reduced to levels comparable to the axial accelerating field gradient. However, this scheme also reduces the acceleration efficiency measures such as r and Q, although r/Q can be comparable to conventional iris-loaded structures. Although the numerical examples of X-band structures are only presented here, we expect that this scheme of reducing ratio of E_s to E_a in a conventional iris-loaded structure at any frequency band can be used by employing partially loaded dielectrics. The fundamental issues about using dielectric loaded structure for particle acceleration, such as dielectric breakdown, Joule heating, and vacuum properties, determine if hybrid dielectric iris-loaded periodic structures can be the alternatives for future linear collider acceleration structures. The experimental investigations on these issues are underway and the advancement in material science also makes this class of structure very promising.

ACKNOWLEDGMENT

This work is supported by US Department of Energy, High Energy Physics Division, Advanced Technology Branch under the Contract No. W-31-109-ENG-38.

[1] P. B. Wilson, Proceedings of 1987 IEEE Particle Accelerator Conference, Washington, D.C., 1987, pp. 53–58.
[2] J. W. Wang *et al.*, Proceedings of the 1999 IEEE Particle Accelerator Conference, New York, 1999, pp. 3423–3425.
[3] M. Dehler *et al.*, Proceedings of the 1997 IEEE Particle Accelerator Conference, Vancouver, Canada, 1997, pp. 518–520.
[4] R. J. Loewen *et al.*, Proceedings of the 1999 IEEE Particle Accelerator Conference, New York, 1999, pp. 3420–3422.
[5] G. Flesher and G. Cohn, AIEE Trans. **70**, 887 (1951).
[6] P. Zou, W. Gai, R. Konecny, X. Sun, T. Wong, and A. Kanareykin, Rev. Sci. Instrum. **71**, 2301 (2000).
[7] T-B. Zhang, J. Hirshfield, T. Marshall, and B. Hafizi, Phys. Rev. E **56**, 4647 (1997).
[8] E. Chjonacki, W. Gai, C. Ho, R. Konecny, S. Mtingwa, J. Norem, M. Rosing, P. Schoessow, and J. Simpson, J. Appl. Phys. **69**, 6257 (1991).
[9] The Los Alamos Accelerator Code Group, Reference Manual for the Poisson/Superfish, LA-UR-87-126, 1987.
[10] MAFIA VERSION 4.0, Gesellschaft fur Computer-Simulationstechnik, Lautschlagerstrabe 38, D-64289, Darmstadt, Germany.
[11] G. A. Loew, R. H. Miller, R. A. Early, and K. L. Bane, IEEE Trans. Nucl. Sci. **NS-26**, 3701 (1979).
[12] T. Wanger, *RF Linear Accelerators* (Wiley, New York, 1998), pp. 23–25.
[13] T. Wanger, *RF Linear Accelerators* (Wiley, New York, 1998), pp. 78–79.
[14] P. Schoessow *et al.*, J. Appl. Phys. **84**, 663 (1998).
[15] S. Gold, private communications.